iScience

CellPress
OPEN ACCESS

Perspective

Understanding the Role of Surface Heterogeneities in Electrosynthesis Reactions

O. Quinn Carvalho,[1] Prajwal Adiga,[1] Sri Krishna Murthy,[1] John L. Fulton,[2] Oliver Y. Gutiérrez,[2] and Kelsey A. Stoerzinger[1,2,*]

SUMMARY

In this perspective, we highlight the role of surface heterogeneity in electrosynthesis reactions. Heterogeneities may come in the form of distinct crystallographic facets, boundaries between facets or grains, or point defects. We approach this topic from a foundation of surface science, where signatures from model systems provide understanding of observations on more complex and higher-surface-area materials. In parallel, probe-based techniques can inform directly on spatial variation across electrode surfaces. We call attention to the role spectroscopy can play in understanding the impact of these heterogeneities in electrocatalyst activity and selectivity, particularly where these surface features have effects extending into the electrolyte double layer.

INTRODUCTION

Electrosynthesis enables the use of (renewable) electrons to drive chemical transformations yielding fuels, chemical precursors, and valuable products. Such reactions rely on electrons transferring to/from intermediates adsorbed on a catalyst surface. The rates of electrosynthesis reactions depend on the local potential of these electrons and the binding strength of intermediates to the catalyst surface. The exposed crystallographic facet of an electrocatalyst controls the coordination number and electron energy levels of active sites (Bondue et al., 2019; Sebastián-Pascual et al., 2019), resulting in so-called *structure-sensitive* activity. This structure sensitivity originates from a minimum "ensemble" of atoms required to accommodate the reactants or products of the reaction or from large disparities among the Gibbs free energy of transition states formed on different kinds of surfaces. Similarly, defects on the electrocatalyst surface, such as vacancies (Gao et al., 2017; Geng et al., 2018), edges (Abbasi et al., 2017), twin boundaries (Li et al., 2017), and grain boundaries (Feng et al., 2015, 2016; Mariano et al., 2017), result in variation of coordination number (Wang et al., 2018), surface strain (Chen et al., 2015; Clark et al., 2017), and electronic structure (Gao et al., 2017; Geng et al., 2018). Their presence can therefore dramatically impact the local activity.

The drive to improve efficiency has emphasized the importance of catalyst design. This requires understanding not only how material composition and crystal structure determine activity but also how heterogeneities in electrocatalysts influence activity. We here focus on the consequences of surface heterogeneity derived from a variety of planes exposed in polycrystalline (electro)catalysts in addition to discussing the presence of steps, kinks, and the boundaries between facets. Studies identifying the role of heterogeneity in electrocatalysis can be broadly classified as those that (1) isolate a desired parameter (e.g., particle size, principle facet orientation, defect structure) in the study of model systems, a so-called surface science approach, or (2) leverage spatially resolved approaches to probe multiple types of heterogeneities on complex surfaces.

We first emphasize the utility of model systems in understanding structure-sensitive reactions (dependence on facet) and their mechanism (spectroscopically determining the mode and extent of adsorption). We next highlight how signatures of these facets can be used to understand the reactivity of polycrystalline systems. Such systems also have grain boundaries and other small length scale heterogeneities such as steps, dislocations, and kinks (Chen et al., 2012), the local properties of which can be addressed by probe-based approaches. Together, these bottom-up and top-down approaches can then inform on the activity of high-surface-area (particle) systems.

[1]School of Chemical, Biological and Environmental Engineering, Oregon State University, 116 Johnson Hall, Corvallis, OR 97331, USA

[2]Institute for Integrated Catalysis, Pacific Northwest National Laboratory, P.O. Box 999, Richland, WA 99352, USA

*Correspondence: kelsey.stoerzinger@oregonstate.edu

https://doi.org/10.1016/j.isci.2020.101814

We will focus our discussion on cathodic electrosynthesis on transition metal catalysts. The most foundational is the generation of hydrogen from water, the hydrogen evolution reaction (HER). More complex reactions, such as the electrochemical hydrogenation (ECH) of organics and the CO_2 reduction reaction (CO2RR) to CO and organics, can sometimes involve elementary aspects of the HER (e.g., when a hydrogen addition step is involved) and/or compete with hydrogen adsorption on the surface. Together, these reactions hold the potential to synthesize an array of value-added products by electrocatalysis, ranging from hydrogen to hydrocarbons and alcohols.

Studies of Model Systems

Crystallographic facets of metals have distinct affinities for adsorption (and subsequent reaction) of hydrogen and organic compounds from aqueous solutions. The study of single crystals can directly access this, although great care must be taken, given the intrinsically low surface area of the system. Although obtaining single crystal samples can be costly, for some systems epitaxial films can be prepared atop an oriented substrate (Hazzazi et al., 2010) to reduce cost and increase throughput. The results obtained from such studies can provide important information in designing high-surface-area systems, discussed in more detail later, and offer an experimental analog to typically modeled systems using, e.g., density functional theory (DFT).

Hydrogen Underpotential Deposition

A prototypical example of a structure-sensitive reaction is the adsorption of protons onto a surface such as platinum at potentials anodic to the HER, termed hydrogen underpotential deposition (H_{upd}). This leads to distinct features in the cyclic voltammogram (CV) of platinum (Clavilier et al., 1980; Climent and Feliu, 2011) due to a larger hydrogen binding energy (Zheng et al., 2015) on the (110) compared with the (100), with that on the (111) being coverage dependent (Figure 1A). The HER is also structure sensitive, with the activity of the (110) facet greater than that of the (100), trending with H_{upd} binding energy, although we note that the relationship between active adsorbed hydrogen and H_{upd} species is complex across facets and electrolytes (Marković et al., 1997; Markovića et al., 1996).

Carbon Dioxide Reduction Reaction

CO2RR activity is well reported to be structure sensitive (Sebastián-Pascual et al., 2019), with product selectivity being material dependent as well. Au and Ag primarily produce CO (in addition to reducing water to form H_2) (Hori, 2017). Undercoordinated sites, such as those on the (110) surface, display higher CO evolution rates on both Ag (Clark et al., 2017; Hoshi et al., 1997; Kolodziej et al., 2018) and Au (Mezzavilla et al., 2019; Todoroki et al., 2019). Cu differs in its ability to produce more reduced carbon species, such as C_2H_4 and CH_4, following CO_2 reduction to CO. Across the low index orientations, C2 products were most prevalent from the (100) orientation (Huang et al., 2017). Fourier transform infrared spectroscopy (FTIR) detected the protonated dimer (COCOH) on Cu (100) but not Cu (111) (Pérez-Gallent et al., 2017a), suggesting (100) sites are responsible for stabilizing adsorbed CO to form the dimer intermediate (Huang et al., 2017; Pérez-Gallent et al., 2017b; Schouten et al., 2013). The C_2H_4/CH_4 ratio can be further increased by the incorporation of (110) and (111) steps onto the surface, provided the (100) terraces are at least four rows in length (Hori et al., 2003; Takahashi et al., 2002). Comparison of yields across Cu single crystals also indicated that under-coordinated sites, such as steps and kinks, promote the formation of alcohols and/or oxygenated species (Bertheussen et al., 2018; Ledezma-Yanez et al., 2016).

Electrochemical Hydrogenation

ECH competes with HER at cathodic potentials, both for active sites and for protons/adsorbed hydrogen atoms in the reduction of organics. Even when such species do not adsorb via an electron transfer process, and thus present no new features in a CV, they can be indirectly observed by displacement of hydrogen and diminishing H_{upd} features. The interaction of organics with a given crystallographic facet depends on the organic functional group. Take, for instance, the ECH of carbonyl compounds on Pt. Acetone is only observed to hydrogenate on the (110) surface but not the (111) and (100) surfaces (Bondue et al., 2019). In contrast, all Pt orientations can hydrogenate the acetyl substituent of acetophenone, but no orientations can hydrogenate 4-acetylpyridine (Bondue and Koper, 2019). This structure sensitivity can first be understood by considering the extent of adsorption via the displacement of H_{upd} features by CV (Figures 1B–1D). Acetone reduces H_{upd} only on the (110) surface, whereas acetophenone reduces H_{upd} on all orientations. However, 4-acetylpyridine also reduces H_{upd}, which indicates that the extent or strength of adsorption alone cannot explain trends in reactivity (Bondue and Koper, 2019). Vibrational spectroscopy can

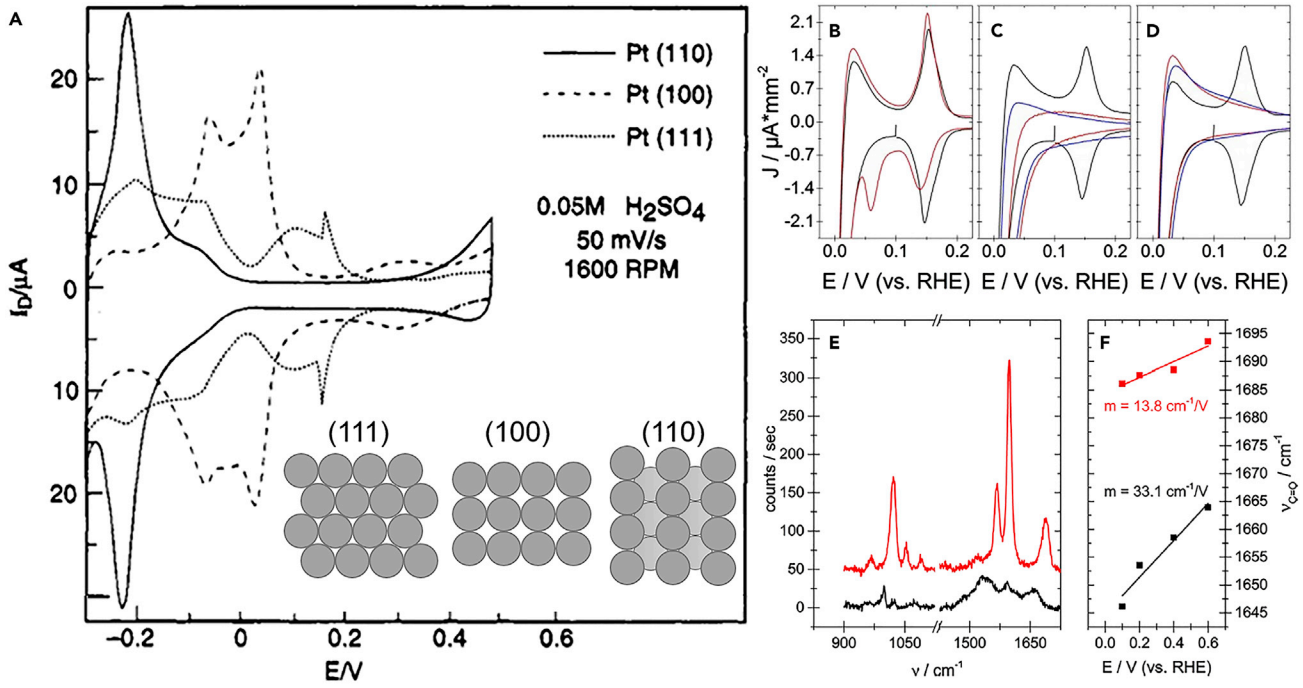

Figure 1. Impact of Pt Orientation on H_{upd}, Displacement of H_{upd} by Organics, and Determining Organic Orientation by Raman Spectroscopy

(A) Cyclic voltammetry of Pt single crystals in oxygen-free electrolyte (V versus SCE); insets show schematics of each plane. Adapted with permission from Markovic et al. (1995). Copyright 1995 American Chemical Society.

(B–D) Comparison of the CV obtained at Pt(110) in the blank electrolyte of 0.1 M H_2SO_4 (black) and in the presence of 0.01 M of the following organic: (B) acetone, (C) acetophenone (red) or benzene (blue), (D) 4-acetylpyridine (red) or pyridine (blue).

(E) SERS spectra for platinum in 0.1 M H_2SO_4 with 0.01 M 4-acetylpyridine (red) or acetophenone (black).

(F) Position of the C—O stretch versus applied potential; the slope (*m*) gives the Stark tuning experienced by the carbonyl functional group.

(B–F) Adapted with permission from https://pubs.acs.org/doi/abs/10.1021/jacs.9b05397 (Bondue and Koper, 2019). Further permissions related to the material excerpted should be directed to the ACS.

probe not only the extent of adsorption but also the orientation of adsorbed organics. Surface-enhanced Raman spectroscopy (SERS) showed that the C-O stretch of the carbonyl group of acetophenone has a greater Stark shift compared with 4-acetylpyridine (Figures 1E and 1F), indicating it is located closer to the electrode surface and experiences a larger change in electric field with polarization. Together with other observed vibrations of the pyridine ring, the lack of 4-acetylpyridine ECH can then be attributed to its vertical adsorption through the N atom, resulting in a carbonyl group far from the surface and insufficiently polarized to be reduced (Bondue and Koper, 2019).

Some small organics can adsorb on metals such as Pt without seemingly affecting the H_{upd} features. The reactivity of distinct facets can be obtained, however, by monitoring desorbed products during a CV. For example, ethene hydrogenates to ethane on the undercoordinated Pt(110) surface, but notably less on the (111) surface, where CVs suggest it adsorbs too strongly to derive any product (Müller et al., 1995). Similarly, benzene hydrogenates completely to cyclohexane on Pt(110), whereas it desorbs mostly unreacted from Pt(100) (Schmiemann and Baltruschat, 1993). Although benzene does not hydrogenate on the (111) surface, the presence of (110) steps leads to hydrogenation. This was confirmed by adsorbing Cu to the steps of Pt(332), which reduces benzene adsorption and dramatically diminishes hydrogenation (Löffler et al., 2003). Together, these studies illustrate that undercoordinated sites on the Pt(110) surface and/or steps have higher reactivity for ECH, although the reactant molecule must adsorb such that the bond to reduce is sufficiently close to the electrocatalyst surface for effective polarization.

Identifying Signatures of Model Systems

With a foundation of surface science-based approaches illustrating signatures of well-defined surfaces, such signatures can then be employed to elucidate the role of facet heterogeneity in polycrystalline

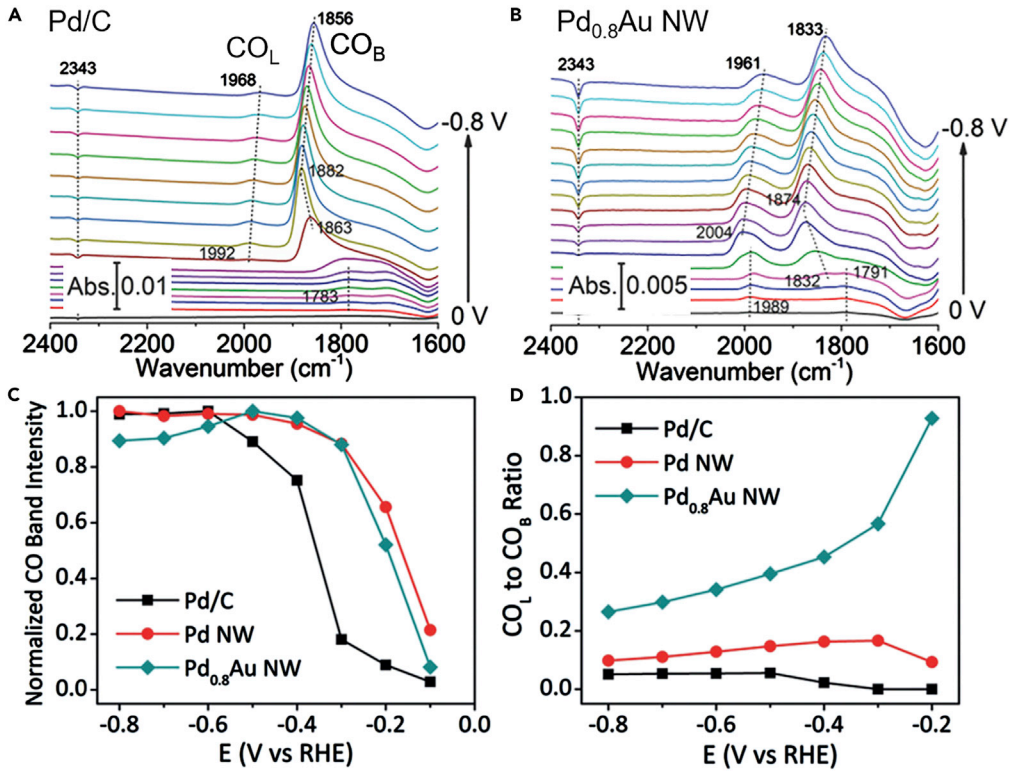

Figure 2. Ratio of Steps and Defects to Terraces Govern Site of CO Adsorption Site and Extent across Potentials

(A and B) Attenuated total reflectance (ATR) FTIR spectra recorded from 0 to −0.8 V versus RHE on (A) Pd nanoparticles, and (B) $Pd_{0.8}Au$ nanowires in CO_2-saturated 0.5 M $KHCO_3$.

(C and D) (C) Normalized total *CO band intensity and (D) CO_L/CO_B (linear/bridged) ratio as a function of applied potentials. Adapted with permission from Zhu et al. (2018). Copyright (2018) WILEY-VCH Verlag GmbH & Co. KGaA, Weinheim.

systems (Vidal-Iglesias et al., 2012). For instance, changes in the facet-dependent H_{upd} features of Pt have been used to determine adsorption energies for organic species like phenol and benzaldehyde. At low coverages, phenol adsorbs only on the Pt(110) and (100) step-like sites but saturates the (111) facets as well at higher coverages. The adsorption enthalpies of phenol, estimated by H_{upd} displacement and modeled as a Frumkin isotherm, were −41 and −21 kJ/mol relative to aqueous phenol for the (110)/(100)-like sites and (111) facets, respectively. In contrast, benzaldehyde has a more negative (higher absolute) heat of adsorption, although demonstrating the same trend with facet orientation as phenol (Singh et al., 2019). The rates, reaction orders, and activation energies for ECH of phenol and benzaldehyde on Pt and other Pt-group metals can be explained well by a Langmuir-Hinshelwood mechanism, with rate-data derived adsorption equilibrium constants for the organics consistent with independently measured values (Singh et al., 2020).

Other sources of electrocatalyst heterogeneity include the specific sites onto which reactants adsorb, which can be identified by vibrational techniques such as FTIR. For example, CO adsorbs at distinct sites on close packed metals: as linear carbonyls at on-top sites, 2-fold coordinated at bridged sites, and 3-fold coordinated at hollow sites. The different binding strengths of CO to the surface lead to observable differences in the C-O stretch frequencies by FTIR. The types of adsorption sites present are further dependent on crystallographic facet: for example, CO primarily adsorbed on hollow sites on Pd(111), bridged sites on Pd(100), and on-top of defects (Groppo et al., 2007). For Pt, FTIR shows that the linear bonding of CO to the (110) surface corresponds to a more facile CO2RR compared with multibonded CO on the (100) face (Rodes et al., 1994a, b). In studying CO2RR on Pd (Figure 2), nanowires adsorbed a higher ratio of linear CO (CO_L) at their copious steps/defects versus bridged CO (CO_B) on terraces compared with nanoparticles with fewer grain boundaries. The linear CO interacts less strongly with the surface, resulting in a lower overpotential for CO2RR (Zhu et al., 2018).

Probe-Based Techniques

In contrast to surface science approaches that simplify systems to understand their constituents, probe-based techniques provide spatial resolution to interrogate heterogeneous surfaces. Such techniques may be employed to identify the local potential in an electric field gradient or probe differences in current density or rate of product generation to identify the active site or the role of defects.

X-ray photoelectron spectroscopy (XPS) is unique in that photoelectrons are sensitive to both the chemical environment and electrostatic potential. Core level photoelectrons are elementally specific and can often distinguish the oxidation state and/or the surrounding ligand environment. For example, ambient pressure XPS (Stoerzinger et al., 2015) was used to study a $CeO_{2-\delta}$ solid oxide electrochemical cell driving the CO2RR. XPS probed the potential profile (Zhang et al., 2012) across a $CeO_{2-\delta}$ catalyst in contact with an Au current collector, identifying the corresponding surface speciation and Ce oxidation state. Carbonate and Ce^{3+} accumulated during CO_2 electrolysis to generate CO over a 400-μm active region on the $CeO_{2-\delta}$ (Yu et al., 2014).

Other approaches probe the potential directly at a conductive tip, such as contact-based potential-sensing electrochemical atomic force microscopy (PS-EC-AFM). In addition to providing local morphology, this technique can directly measure the surface electrochemical potential in heterogeneous electrochemical systems. PS-EC-AFM has recently been demonstrated to observe the potential- and thickness-dependent electronic properties of cobalt (oxy)hydroxide phosphate (CoPi) on illuminated hematite (α-Fe_2O_3) photoelectrodes (Nellist et al., 2018).

With sufficient resolution (on the atomic scale), probe-based techniques can identify active sites, such as edges or other heterogeneities. Scanning tunneling microscopy (STM) can measure surface reactivity (convoluted with morphology) by the tunneling current. In addition, highly active sites result in electrochemical noise due to changes in electrolyte composition and local ad/desorption processes (Figure 3). This approach has been used to probe the active sites for the HER, demonstrating that for Pt in acid, step edges are much more active than (111) terraces (Pfisterer et al., 2017). In contrast, for metals supported on Au(111), Pt terrace sites are active, whereas Pd atoms at the boundary are more active than those at the center of Pd islands (Figure 3) (Liang et al., 2019).

Other probe-based techniques that operate at greater length scales can detect an increase in local activity near defects such as grain boundaries (Mariano et al., 2017). Scanning electrochemical cell microscopy (SECM) has shown that the increased catalytic activity of Au grain boundaries for CO_2 and CO reduction is on a length scale (0.5–4 μm), commensurate with its dislocation-induced strain field (Mariano et al., 2017). Dislocation-induced strain may alter reaction intermediate binding energy and/or create high step densities with greater activity than terrace sites. Small probes can also be polarized to locally detect products (such as evolved H_2 via its oxidation), measuring local activity by the current passed between the probe and the sample. This technique has been used to identify size-dependent nanoparticle activity for HER by an electrochemical STM (Meier et al., 2002) and an SECM tip (Sun et al., 2014).

Correlations in Nanoparticle and Polycrystalline Systems

Building off the findings from surface science- and probe-based techniques, high-surface-area systems can also be studied to look for correlations in catalyst activity, material properties, and reactant adsorption. For structure-sensitive reactions, studies have considered relations between particle size or shape, the expected ratio of facets:edges (Figure 4), and catalytic activity or selectivity.

The ECH of phenol and benzaldehyde has been studied for Pt nanoparticles ranging in size. The intrinsic activity of Pt, measured by the turnover frequency (TOF), increased with the size of Pt particles, which matched the increase of the fraction of planar sites, Pt(100) and Pt(111) according to geometric models. Interestingly, the same trend was observed for both molecules despite hydrogenation of different functional groups, i.e., the aromatic ring in phenol and the carbonyl group in benzaldehyde (without ring hydrogenation). The higher activity of planar sites was attributed to stronger adsorption of the organic compounds on those planes. This hypothesis was verified by exposing different sized catalyst nanoparticles to cathodic potentials (to generate adsorbed hydrogen) with and without phenol to compare the changes in the Pt-H signal in X-ray absorption near edge spectroscopy (XANES) (i.e., the hydrogen displaced by the organic compound) (Sanyal et al., 2019). The largest change was observed for the catalyst with the largest

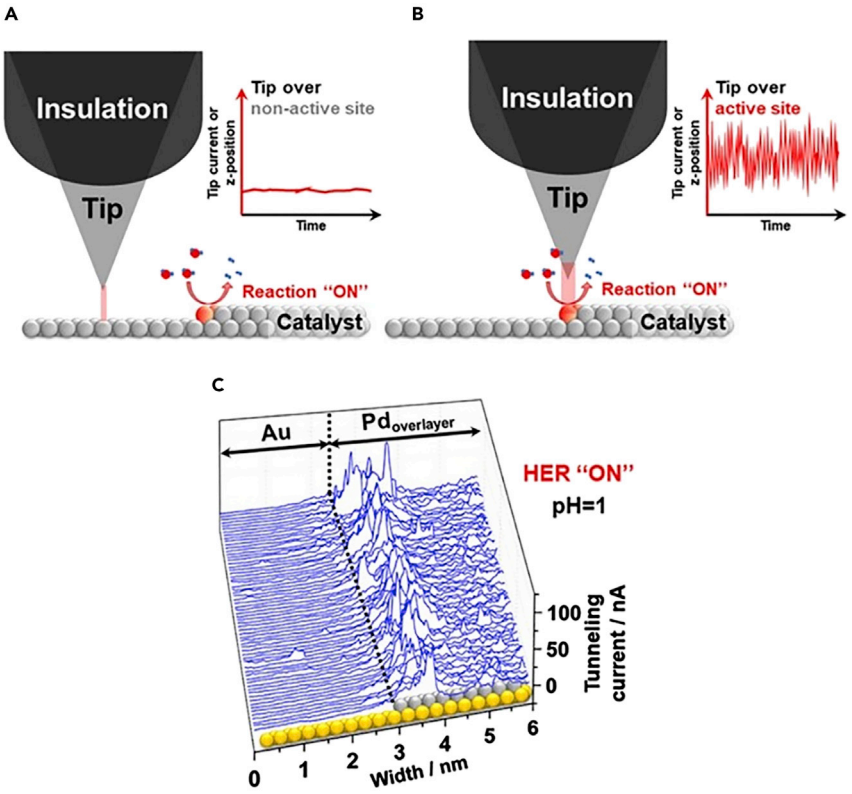

Figure 3. STM Can Identify Active Sites by Electrochemical Noise in the Tunneling Current

(A and B) A scheme explaining how local changes in environment alter the tunneling barrier in STM. Increased tunneling-current noise is likely when the tip is over a more active step edge (B), compared with terrace sites (A).

(C) STM line scans across Au-supported Pd islands under HER conditions in 0.1 M H_2SO_4. Pd atoms at the boundary are more active than atoms at the center of Pd islands. Reprinted with permission from Liang et al. (2019). Copyright (2019) American Chemical Society.

particle size, in agreement with the hypothesis that active planar sites strongly adsorb organic and displace hydrogen. A follow-up study applied the same principle of displacing adsorbed H from a polycrystalline Pt electrode with organics, but the displacement was monitored by CV (Singh et al., 2019). These trends in ECH can be further understood by considering particle size effects on the competing HER. Similar to studies of Pt single crystals identifying steps as highly active for HER (Pfisterer et al., 2017), the edges and vertices of Pt nanoparticles have been suggested to be much more active for HER than facets (Zalitis et al., 2017), consistent with the dominance of ECH on large particles with a larger fraction of planar sites (Sanyal et al., 2019).

Nanoparticle shape also influences the exposed facets. The hydrogenation of 2-cyclohexenone on Pt particles of different shapes showed similar rates on cubes (with exposed (100) planes) and cuboctahedra (with exposed (100) and (111) planes); however, the ratio of 4:2 electron products (cyclohexanol:cyclohexanone) was three times lower on cubes than on cuboctahedra (Kim and Lee, 2009). The latter points to better hydrogenation activity of the mixture of (100) and (111) in cuboctahedra than of pure (100) planes.

In agreement with studies on single crystals for the CO2RR, Cu nanocubes with a high fraction of (100) facets are more selective toward C_2H_4 production compared with nanoparticles with an array of different surface sites (Loiudice et al., 2016; Roberts et al., 2015). Minimizing the competing HER reaction, however, requires simultaneous optimization of the type of exposed facet and extent of under-coordinated sites at cube edges by, e.g., changing cube size (Loiudice et al., 2016).

Polycrystalline surfaces and nanoparticles not only display a variety of facets with distinct properties but also have undercoordinated sites and strain fields where different facets or orientations of the same facet

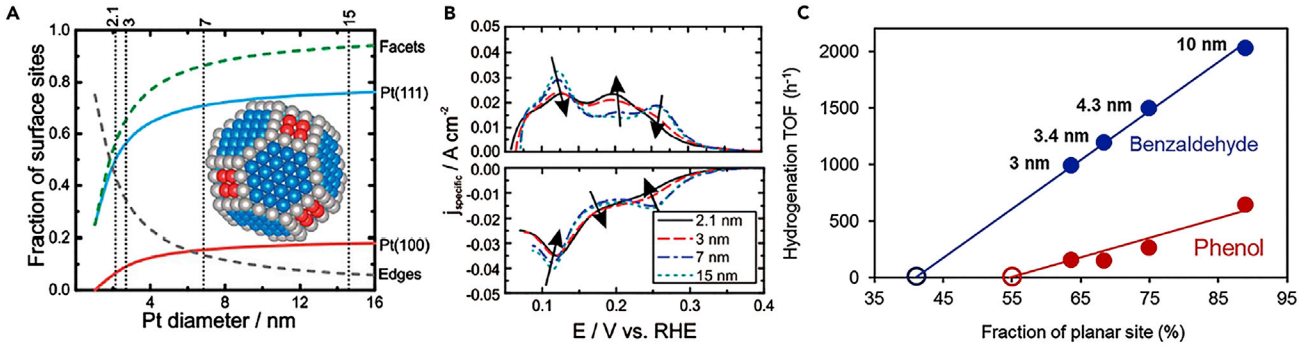

Figure 4. Particle Size Influences Fraction of Exposed Planes, H_{upd}, and ECH Activity

(A) Fraction of Pt(111), Pt(100), edge and facet (Pt(111) + Pt(100)) sites on Pt cubo-octahedron particles (Zalitis et al., 2017). Published by The Royal Society of Chemistry.

(B) Electrochemical response in 4 M $HClO_4$ of different-sized platinum particles. Arrows show the transition from a larger to a smaller particle size with more (111) facets (Zalitis et al., 2017). Published by The Royal Society of Chemistry.

(C) Turnover frequencies observed for the ECH of benzaldehyde and phenol (at −0.7 V versus Ag/AgCl) over a series of Pt catalysts with different particle sizes. The x axis shows the fraction of (100) and (111) terrace sites corresponding to those nanoparticle sizes. Reprinted with permission from Sanyal et al. (2019). Copyright (2020) WILEY-VCH Verlag GmbH & Co. KGaA, Weinheim.

join. These grain boundaries can also influence electrocatalyst activity and selectivity. The role of grain boundaries has been extensively investigated for the CO2RR. Multiple reports found correlation between increasing grain boundary density on Au and Cu electrodes and increasing activity for the CO2RR and the related CO reduction reaction (Feng et al., 2015, 2016). Considering a range of twin boundary densities on Cu, the TOF for CH_4 production on the twin boundary atoms was determined to be three orders of magnitude higher than on plane atoms (Tang et al., 2020).

Opportunities in Electrosynthesis

Current gaps in understanding the effect of electrode heterogeneity for electrosynthesis offer opportunities to improve catalyst design for activity and selectivity. Considering the hydrogenation of carbon-containing species in ECH and CO2RR, missing is an understanding of how carbon species and hydrogen (protons) compete for adsorption on particles with a variety of planes and edges, and how this competition is influenced by species in the electric double layer (including water). Such understanding holds the potential to optimize the pathways of the targeted transformations. Spectroscopic approaches can identify and sometimes quantify adsorbed species, where the signatures of these adsorbates are often characteristic of the coordination environment (e.g., crystallographic facet, extent of bonding) on heterogeneous catalyst surfaces. These spectroscopic approaches may be leveraged further by probing the effect of surface heterogeneities on electrolyte, and vice versa. Resulting insights would provide a greater understanding of the critical solid-electrolyte interface, e.g., cation hydration shell effects, selective anion adsorption, and local pH. This understanding would guide the design not only of catalyst surfaces and their heterogeneities but the reaction environment as well.

X-ray techniques, although often penetrating through the entire bulk of an electrocatalyst, can still assess adsorbed species owing to elemental sensitivity. Owing to the bulk sensitivity of transmission- and fluorescence-based X-ray absorption studies, electrosynthesis studies are typically limited to catalyst particles where a significant fraction of the atoms are located at the surface (characteristic of particles less than about 2 nm). X-ray absorption features arise from two processes: XANES and EXAFS. XANES involves electron excitation from core to bound states, whereas extended X-ray absorption fine structure (EXAFS) involves scattering of the photoelectron by neighboring atoms. For XANES, sensitivity to surface species can be greatly enhanced by subtracting contributions from the non-reactive particle core atoms. Recent theory advances can quantitatively predict XANES spectra. For instance, time-dependent DFT (TD-DFT), which captures the excited electronic states observed in XANES (Lopata et al., 2012), enables characterization of molecular species at active metal sites under electrochemical conditions. Both X-ray absorption techniques hold promise for future use in assessing competition between C and H species on metals in operating conditions, and comparison of select systems (e.g., particles of different size) can elucidate the role of

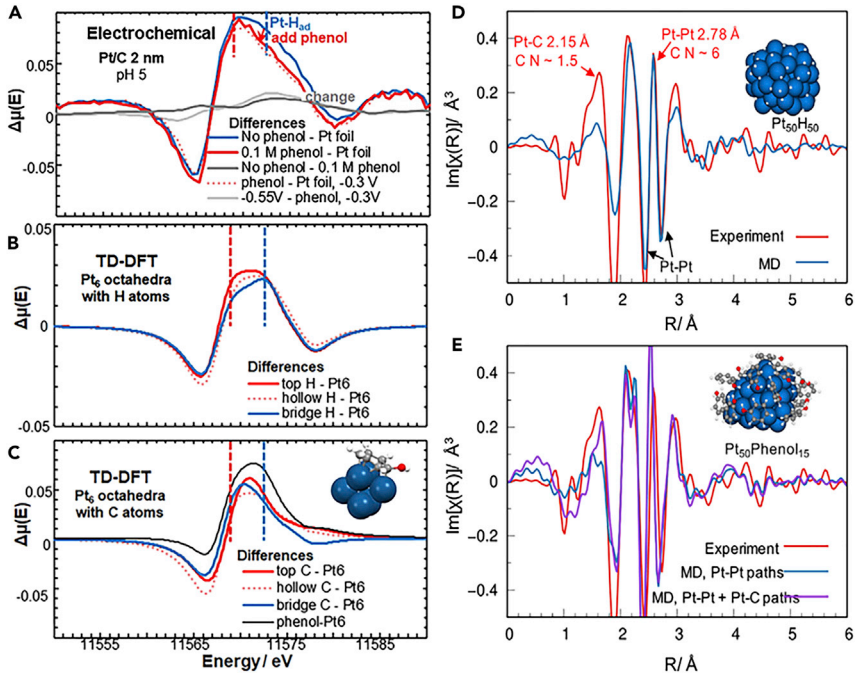

Figure 5. X-ray Absorption and Theory Probe the Competition between Organics and Hydrogen during ECH

(A) XANES Pt L_3-edge difference spectra in 3 M acetate buffer; potentials are versus Ag/AgCl.

(B) TD-DFT XANES difference spectra for a Pt_6 cluster having a single hydrogen atom adsorbed minus the spectrum for a bare cluster.

(C) TD-DFT XANES difference spectra for phenol adsorbed through a carbon atom at top, hollow or bridge sites.

(D and E) Experimental and simulated EXAFS radial structure plots as Im[χ(R)]. The computed molecular dynamics extended X-ray absorption fine structure (MD-EXAFS) is for a 50 atom Pt cluster with adsorbed hydrogen (Pt:H = 1, (D)) or adsorbed phenol (50 Pt atoms and 15 phenol molecules, (E)). The MD-EXAFS in (E) is shown considering only Pt-Pt paths or also including Pt-C (C of phenol molecules). The corresponding models are shown in the figures. Adapted from Singh et al. (2018) with permission from Elsevier.

defects like grain boundaries and edges in competitive adsorption and reaction during electrosynthesis reactions.

Coupling *ab initio* simulations with X-ray absorption spectroscopy can identify carbon-metal interactions as a function of applied potential (Figure 5). For phenol under electrosynthesis conditions, theoretical calculations suggest that the aromatic ring of adsorbed phenol (subsequently reduced) lies parallel to the Pt surface as confirmed by XANES experiments. XANES difference methods further illustrate the competition at the bridge sites for either C (phenol) or H adsorption. Theory additionally shows H binds at corner and edge sites of Pt nanoparticles that do not optimally bind phenol, and X-ray absorption shows the persistence of adsorbed H under ECH conditions (Singh et al., 2018). EXAFS probes bond lengths and coordination numbers. The predicted Pt-C bond lengths for phenol on platinum nanoparticles are in agreement with measurements using EXAFS (Figure 5D).

Other X-ray techniques, such as XPS, offer more sensitivity to surface adsorbates. Although XPS has typically been limited to ultra-high vacuum on account of the low kinetic energy of surface-sensitive photoelectrons, the technique has recently been adapted to operate at ambient pressure (AP-XPS) (Eren et al., 2016; Stoerzinger et al., 2015; Yu et al., 2014; Zhang et al., 2012) and even with liquid electrolyte (Favaro et al., 2016; Stoerzinger et al., 2018). This enables determination of surface stoichiometry and oxidation state under operating conditions (Yu et al., 2014; Zhang et al., 2012), and even provides adsorbate speciation (Stoerzinger et al., 2018) and information about the double layer (Favaro et al., 2016). For example, AP-XPS has detected *OH and *H remain on the surface of a porous Pt electrode during HER in alkaline electrolyte (Stoerzinger et al., 2018). The Pt-H component persisted after oxidative stripping, suggesting the porous structure may impact local pH and electric field gradients. AP-XPS can also probe the local voltage

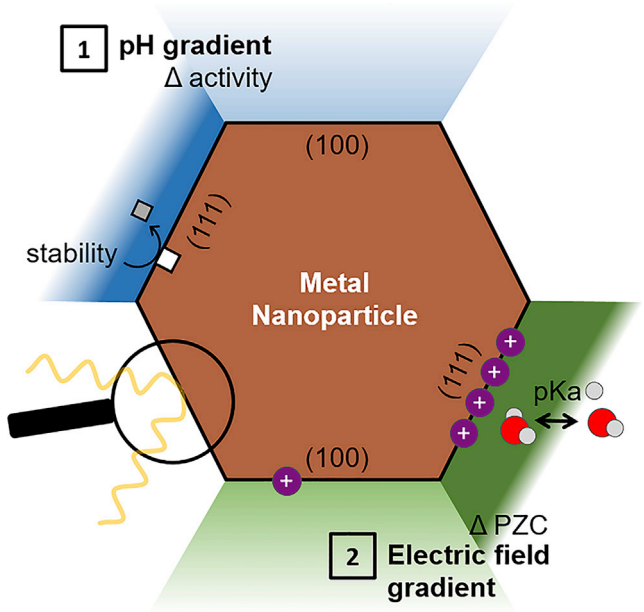

Figure 6. Schematic of How Opportunities in Spectroscopy Can Inform on the Impact of Surface Heterogeneity-Double Layer Interaction on Activity

Here, we provide an illustrated example of the heterogeneous facets of a hexagonal metal nanoparticle interacting differently with the surrounding electrolyte, providing facet-dependent variation of the pH gradient, electric field gradient, reactant and product mass transfer, and coupled catalyst properties such as stability.

drop in the electrochemical double layer by the binding energy of photoelectrons (Favaro et al., 2016), which may vary with surface roughness (Daikhin et al., 1997) or exposed crystallographic facet due to variation in local pH (coupled to differences in activity/selectivity).

Vibrational spectroscopies, such as FTIR and Raman, have recently been employed to deduce the extent and mode of adsorption for organic species. These techniques can be performed during electrode polarization to further identify the potentials of adsorption and conversion (Malkani et al., 2020), including information on the polarization experienced by a given bond due to the electric field gradient (Bondue and Koper, 2019). Operando vibrational spectroscopy can further identify intermediate species that form at a specific polarization (Pérez-Gallent et al., 2017a). For the ECH of benzaldehyde, a ketyl radical was identified to mediate the electrocatalytic reduction of benzaldehyde to hydrobenzoin on Au and Cu by attenuated total reflection surface-enhanced infrared reflection absorption spectroscopy (ATR-SEIRAS) (Anibal et al., 2020). Interestingly, the authors reported the formation of CO associated with the adsorption of benzaldehyde on Pt, which could have important consequences for the stability of Pt electrodes or, as seen from single crystal studies, the stability of some Pt planes.

Although vibrational spectroscopies can be surface sensitive (Zhu et al., 2019), the evanescent field employed in such techniques extends into the double layer and electrolyte as well, providing insight into the reaction products, local pH, and salt effects. This has recently brought great insight into the CO2RR. The pH buffering effect of bicarbonate anions in CO2RR electrolyte has been observed by FTIR (Zhu et al., 2017), and the local pH can be quantified by measuring the carbonate/bicarbonate band area ratio (Dunwell et al., 2018). These bicarbonate ions have further been shown by FTIR to be the primary CO_2 source and mediators during the CO2RR (Zhu et al., 2017). Thus, local differences in activity at heterogeneous surfaces may be compounded by effective CO_2 concentrations as well. FTIR has also demonstrated that the size of cations can impact the local pH, attributed to a decrease in the pKa of hydrolysis due to the polarization of water between the cation and negatively charged electrode (Ayemoba and Cuesta, 2017).

As illustrated for the CO2RR above, the impact of catalyst heterogeneities (shown in Figure 6 as different facets) may extend beyond the surface and into the electrolyte double layer, further affecting the activity and selectivity in electrosynthesis reactions. For reactions consuming/generating protons (such as HER

and hydrogenation reactions discussed here), variations in facet activity can lead to distinct pH gradients, which may affect catalyst stability and even shape. For example, a facet that more rapidly consumes protons may have a locally higher pH than a less active facet, driving the former's selective dissolution if soluble in alkaline conditions. FTIR can provide insight into this process by probing local pH gradients through band area ratios of buffer components. Inherent differences in the work function and potential of zero charge (PZC) of crystallographic facets (and the logical extension to steps as well) (Gómez et al., 2000) can also result in different surface charges under applied potential and corresponding variation in adsorption of nearby ions. The resultant differences in local electric field can influence the bond polarization of adsorbates (Hussain et al., 2019), and subsequently the activity and selectivity of a facet, even leading to local variation in the pKa of solvent molecules, again affecting local pH. Techniques like FTIR and Raman can probe bond polarization through Stark shifts, and ambient pressure XPS accesses electric fields and salt concentrations through the binding energy and intensity of emitted photoelectrons. Variation in both pH and electric field gradients, observable by spectroscopic approaches, may provide further explanation of how the rates and selectivity of an electrocatalyst depend on exposed facet and the presence of other heterogeneities (such as grain boundaries, steps, kinks).

CONCLUSION

We have highlighted examples where surface heterogeneities impact catalyst activity and selectivity in electrosynthesis reactions. Building off a foundation of surface science approaches, the study of model systems can provide signatures for understanding the behavior of more complex catalysts with multiple exposed facets and grain boundaries, such as cyclic voltammetry features corresponding to H adsorption on distinct facets. Probe-based techniques can isolate the contribution of some heterogeneities to electrocatalyst activity, such as active step edges for HER on Pt or strained grain boundaries for the CO2RR on Cu. These approaches to isolate parameters, either in model systems or via spatial resolution, build explicit understanding and bolster observed correlations between material parameters and catalyst performance in nanoparticle and polycrystalline systems, such as size and shape-dependent activity and selectivity. We further highlight how spectroscopy can elucidate the role of heterogeneities in cathodic electrosynthetic reactions. X-ray and vibrational spectroscopies can assess competitive adsorption between C and H species at the catalyst surface and further probe how catalyst heterogeneities impact the electrolyte double layer. The use of such approaches can further develop the underlying physicochemical principles dictating (electro)catalyst activity and selectivity, guiding the design of stable catalysts down to the level of exposed crystallographic facet and heterogeneous defect (e.g., step edge, grain boundary) density.

ACKNOWLEDGMENTS

O.Y.G., J.L.F., and K.A.S. are part of the Chemical Transformation Initiative at Pacific Northwest National Laboratory (PNNL), a Laboratory Directed Research and Development Program at PNNL, a multiprogram national laboratory operated by Battelle for the US Department of Energy under Contract No. DE-AC05-76RL01830. Acknowledgment is made to the donors of the American Chemical Society Petroleum Research Fund for partial support of this work. K.A.S. acknowledges support from Oregon State University as a Callahan Faculty Scholar. P.A. acknowledges support from the Link Foundation Energy Fellowship.

AUTHOR CONTRIBUTIONS

Conceptualization, K.A.S.; Investigation, O.Q.C., O.Y.G., and K.A.S.; Writing – Original Draft, O.Q.C., O.Y.G., and K.A.S.; Writing – Review & Editing, O.Q.C., P.A., S.K.M., J.L.F., O.Y.G., and K.A.S.; Funding Acquisition, O.Y.G. and K.A.S.

REFERENCES

Abbasi, P., Asadi, M., Liu, C., Sharifi-Asl, S., Sayahpour, B., Behranginia, A., Zapol, P., Shahbazian-Yassar, R., Curtiss, L.A., and Salehi-Khojin, A. (2017). Tailoring the edge structure of molybdenum disulfide toward electrocatalytic reduction of carbon dioxide. ACS Nano *11*, 453–460.

Anibal, J., Malkani, A., and Xu, B. (2020). Stability of the ketyl radical as a descriptor in the electrochemical coupling of benzaldehyde. Catal. Sci. Technol. *10*, 3181–3194.

Ayemoba, O., and Cuesta, A. (2017). Spectroscopic evidence of size-dependent buffering of interfacial pH by cation hydrolysis during CO_2 electroreduction. ACS Appl. Mater. Interfaces *9*, 27377–27382.

Bertheussen, E., Hogg, T.V., Abghoui, Y., Engstfeld, A.K., Chorkendorff, I., and Stephens, I.E.L. (2018). Electroreduction of CO on polycrystalline copper at low overpotentials. ACS Energy Lett. *3*, 634–640.

Bondue, C.J., Calle-Vallejo, F., Figueiredo, M.C., and Koper, M.T.M. (2019). Structural principles to steer the selectivity of the electrocatalytic reduction of aliphatic ketones on platinum. Nat. Catal. *2*, 243–250.

Bondue, C.J., and Koper, M.T.M. (2019). Electrochemical reduction of the carbonyl functional group: the importance of adsorption geometry, molecular structure, and electrode surface structure. J. Am. Chem. Soc. *141*, 12071–12078.

Chen, Q.-S., Vidal-Iglesias, F.J., Solla-Gullón, J., Sun, S.-G., and Feliu, J.M. (2012). Role of surface defect sites: from Pt model surfaces to shape-controlled nanoparticles. Chem. Sci. *3*, 136–147.

Chen, Z., Zhang, X., and Lu, G. (2015). Overpotential for CO_{-2} electroreduction lowered on strained penta-twinned Cu nanowires. Chem. Sci. *6*, 6829–6835.

Clark, E.L., Hahn, C., Jaramillo, T.F., and Bell, A.T. (2017). Electrochemical CO_{-2} reduction over compressively strained CuAg surface alloys with enhanced multi-carbon oxygenate selectivity. J. Am. Chem. Soc. *139*, 15848–15857.

Clavilier, J., Faure, R., Guinet, G., and Durand, R. (1980). Preparation of monocrystalline Pt microelectrodes and electrochemical study of the plane surfaces cut in the direction of the {111} and {110} planes. J. Electroanal. Chem. Interfacial Electrochem. *107*, 205–209.

Climent, V., and Feliu, J.M. (2011). Thirty years of platinum single crystal electrochemistry. J. Solid State Electrochem. *15*, 1297.

Daikhin, L.I., Kornyshev, A.A., and Urbakh, M. (1997). Double layer capacitance on a rough metal surface: surface roughness measured by "Debye ruler". Electrochimica Acta *42*, 2853–2860.

Dunwell, M., Yang, X., Setzler, B.P., Anibal, J., Yan, Y., and Xu, B. (2018). Examination of near-electrode concentration gradients and kinetic impacts on the electrochemical reduction of CO_2 using surface-enhanced infrared spectroscopy. ACS Catal. *8*, 3999–4008.

Eren, B., Weatherup, R.S., Liakakos, N., Somorjai, G.A., and Salmeron, M. (2016). Dissociative carbon dioxide adsorption and morphological changes on Cu(100) and Cu(111) at ambient pressures. J. Am. Chem. Soc. *138*, 8207–8211.

Favaro, M., Jeong, B., Ross, P.N., Yano, J., Hussain, Z., Liu, Z., and Crumlin, E.J. (2016). Unravelling the electrochemical double layer by direct probing of the solid/liquid interface. Nat. Commun. *7*, 12695.

Feng, X., Jiang, K., Fan, S., and Kanan, M.W. (2015). Grain-boundary-dependent CO_2 electroreduction activity. J. Am. Chem. Soc. *137*, 4606–4609.

Feng, X., Jiang, K., Fan, S., and Kanan, M.W. (2016). A direct grain-boundary-activity correlation for CO electroreduction on Cu nanoparticles. ACS Cent. Sci. *2*, 169–174.

Gao, S., Sun, Z., Liu, W., Jiao, X., Zu, X., Hu, Q., Sun, Y., Yao, T., Zhang, W., Wei, S., et al. (2017). Atomic layer confined vacancies for atomic-level insights into carbon dioxide electroreduction. Nat. Commun. *8*, 14503.

Geng, Z., Kong, X., Chen, W., Su, H., Liu, Y., Cai, F., Wang, G., and Zeng, J. (2018). Oxygen vacancies in ZnO nanosheets enhance CO_2 electrochemical reduction to CO. Angew. Chem. Int. Ed. *57*, 6054–6059.

Gómez, R., Climent, V., Feliu, J.M., and Weaver, M.J. (2000). Dependence of the potential of zero charge of stepped platinum (111) electrodes on the oriented step-edge Density: electrochemical implications and comparison with work function behavior. J. Phys. Chem. B *104*, 597–605.

Groppo, E., Bertarione, S., Rotunno, F., Agostini, G., Scarano, D., Pellegrini, R., Leofanti, G., Zecchina, A., and Lamberti, C. (2007). Role of the support in determining the vibrational properties of carbonyls formed on Pd supported on SiO_2–Al_2O_3, Al_2O_3, and MgO. J. Phys. Chem. C *111*, 7021–7028.

Hazzazi, O.A., Huxter, S.E., Taylor, R., Palmer, B., Gilbert, L., and Attard, G.A. (2010). Electrochemical studies of irreversibly adsorbed ethyl pyruvate on Pt{hkl} and epitaxial Pd/Pt{hkl} adlayers. J. Electroanalytical Chem. *640*, 8–16.

Hori, Y. (2017). Modern Aspects of Electrochemistry, *vol. 42* (Springer).

Hori, Y., Takahashi, I., Koga, O., and Hoshi, N. (2003). Electrochemical reduction of carbon dioxide at various series of copper single crystal electrodes. J. Mol. Catal. A: Chem. *199*, 39–47.

Hoshi, N., Kato, M., and Hori, Y. (1997). Electrochemical reduction of CO_2 on single crystal electrodes of silver Ag(111), Ag(100) and Ag(110). J. Electroanalytical Chem. *440*, 283–286.

Huang, Y., Handoko, A.D., Hirunsit, P., and Yeo, B.S. (2017). Electrochemical reduction of CO_2 using copper single-crystal surfaces: effects of CO* coverage on the selective formation of ethylene. ACS Catal. *7*, 1749–1756.

Hussain, G., Pérez-Martínez, L., Le, J.-B., Papasizza, M., Cabello, G., Cheng, J., and Cuesta, A. (2019). How cations determine the interfacial potential profile: relevance for the CO_2 reduction reaction. Electrochimica Acta *327*, 135055.

Kim, C., and Lee, H. (2009). Shape effect of Pt nanocrystals on electrocatalytic hydrogenation. Catal. Commun. *11*, 7–10.

Kolodziej, A., Rodriguez, P., and Cuesta, A. (2018). Chapter 4 single-crystal surfaces as model electrocatalysts for CO_2 reduction. In Electrochemical Reduction of Carbon Dioxide: Overcoming the Limitations of Photosynthesis, F. Marken and D. Fermin, eds. ((The Royal Society of Chemistry)), pp. 88–110.

Ledezma-Yanez, I., Gallent, E.P., Koper, M.T.M., and Calle-Vallejo, F. (2016). Structure-sensitive electroreduction of acetaldehyde to ethanol on copper and its mechanistic implications for CO and CO_2 reduction. Catal. Today *262*, 90–94.

Li, Y., Cui, F., Ross, M.B., Kim, D., Sun, Y., and Yang, P. (2017). Structure-sensitive CO_2 electroreduction to hydrocarbons on Ultrathin 5-fold twinned copper nanowires. Nano Lett. *17*, 1312–1317.

Liang, Y., Csoklich, C., McLaughlin, D., Schneider, O., and Bandarenka, A.S. (2019). Revealing active sites for hydrogen evolution at Pt and Pd atomic layers on Au surfaces. ACS Appl. Mater. Interfaces *11*, 12476–12480.

Löffler, T., Bussar, R., Drbalkova, E., Janderka, P., and Baltruschat, H. (2003). The role of mono-atomic steps and of step decoration by Cu on the adsorption and hydrogenation of benzene and cyclohexene on Pt single crystal electrodes. Electrochimica Acta *48*, 3829–3839.

Loiudice, A., Lobaccaro, P., Kamali, E.A., Thao, T., Huang, B.H., Ager, J.W., and Buonsanti, R. (2016). Tailoring copper nanocrystals towards C2 products in electrochemical CO_2 reduction. Angew. Chem. Int. Ed. *55*, 5789–5792.

Lopata, K., Van Kuiken, B.E., Khalil, M., and Govind, N. (2012). Linear-response and real-time time-dependent density functional theory studies of core-level near-edge X-ray absorption. J. Chem. Theor. Comput. *8*, 3284–3292.

Malkani, A.S., Anibal, J., Chang, X., and Xu, B. (2020). Bridging the gap in the mechanistic understanding of electrocatalysis via in-situ characterizations. iScience *23*, 101776.

Mariano, R.G., McKelvey, K., White, H.S., and Kanan, M.W. (2017). Selective increase in CO_2 electroreduction activity at grain-boundary surface terminations. Science *358*, 1187–1192.

Markovic, N.M., Gasteiger, H.A., and Ross, P.N. (1995). Oxygen reduction on platinum low-index single-crystal surfaces in Sulfuric acid solution: rotating ring-Pt(hkl) disk studies. J. Phys. Chem. *99*, 3411–3415.

Marković, N.M., Grgur, B.N., and Ross, P.N. (1997). Temperature-dependent hydrogen electrochemistry on platinum low-index single-crystal surfaces in acid solutions. J. Phys. Chem. B *101*, 5405–5413.

Markovića, N.M., Sarraf, S.T., Gasteiger, H.A., and Ross, P.N. (1996). Hydrogen electrochemistry on platinum low-index single-crystal surfaces in alkaline solution. J. Chem. Soc. Faraday Trans. *92*, 3719–3725.

Meier, J., Friedrich, K.A., and Stimming, U. (2002). Novel method for the investigation of single nanoparticle reactivity. Faraday Discuss. *121*, 365–372.

Mezzavilla, S., Horch, S., Stephens, I.E.L., Seger, B., and Chorkendorff, I. (2019). Structure sensitivity in the electrocatalytic reduction of CO_2 with Gold catalysts. Angew. Chem. Int. Ed. *58*, 3774–3778.

Müller, U., Schmiemann, U., Dülberg, A., and Baltruschat, H. (1995). Adsorption and hydrogenation of simple alkenes at Pt-group metal electrodes studied by DEMS: influence of the crystal orientation. Surf. Sci. *335*, 333–342.

Nellist, M.R., Laskowski, F.A.L., Qiu, J., Hajibabaei, H., Sivula, K., Hamann, T.W., and Boettcher, S.W. (2018). Potential-sensing electrochemical atomic force microscopy for in operando analysis of water-splitting catalysts and interfaces. Nat. Energy *3*, 46–52.

Pérez-Gallent, E., Figueiredo, M.C., Calle-Vallejo, F., and Koper, M.T.M. (2017a). Spectroscopic observation of a hydrogenated CO dimer intermediate during CO reduction on Cu(100) electrodes. Angew. Chem. Int. Ed. *56*, 3621–3624.

Pérez-Gallent, E., Marcandalli, G., Figueiredo, M.C., Calle-Vallejo, F., and Koper, M.T.M. (2017b). Structure- and potential-dependent cation effects on CO reduction at copper single-crystal electrodes. J. Am. Chem. Soc. *139*, 16412–16419.

Pfisterer, J.H.K., Liang, Y., Schneider, O., and Bandarenka, A.S. (2017). Direct instrumental

identification of catalytically active surface sites. Nature *549*, 74–77.

Roberts, F.S., Kuhl, K.P., and Nilsson, A. (2015). High selectivity for ethylene from carbon dioxide reduction over copper nanocube electrocatalysts. Angew. Chem. Int. Ed. *54*, 5179–5182.

Rodes, A., Pastor, E., and Iwasita, T. (1994a). Structural effects on CO_2 reduction at Pt single-crystal electrodes: Part 1. The Pt(110) surface. J. Electroanalytical Chem. *369*, 183–191.

Rodes, A., Pastor, E., and Iwasita, T. (1994b). Structural effects on CO_2 reduction at Pt single-crystal electrodes: Part 3. Pt(100) and related surfaces. J. Electroanalytical Chem. *377*, 215–225.

Sanyal, U., Song, Y., Singh, N., Fulton, J.L., Herranz, J., Jentys, A., Gutiérrez, O.Y., and Lercher, J.A. (2019). Structure sensitivity in hydrogenation reactions on Pt/C in aqueous-phase. ChemCatChem *11*, 575–582.

Schmiemann, U., and Baltruschat, H. (1993). The influence of the single-crystal orientation on the electrocatalytic hydrogenation of benzene and the H•D exchange. J. Electroanalytical Chem. *347*, 93–109.

Schouten, K.J.P., Pérez Gallent, E., and Koper, M.T.M. (2013). Structure sensitivity of the electrochemical reduction of carbon monoxide on copper single crystals. ACS Catal. *3*, 1292–1295.

Sebastián-Pascual, P., Mezzavilla, S., Stephens, I.E.L., and Escudero-Escribano, M. (2019). Structure-sensitivity and electrolyte effects in CO_2 electroreduction: from model studies to applications. ChemCatChem *11*, 3626–3645.

Singh, N., Nguyen, M.-T., Cantu, D.C., Mehdi, B.L., Browning, N.D., Fulton, J.L., Zheng, J., Balasubramanian, M., Gutiérrez, O.Y., Glezakou, V.-A., et al. (2018). Carbon-supported Pt during aqueous phenol hydrogenation with and without applied electrical potential: X-ray absorption and theoretical studies of structure and adsorbates. J. Catal. *368*, 8–19.

Singh, N., Sanyal, U., Fulton, J.L., Gutiérrez, O.Y., Lercher, J.A., and Campbell, C.T. (2019). Quantifying adsorption of organic molecules on platinum in aqueous phase by hydrogen site blocking and in situ X-ray absorption spectroscopy. ACS Catal. *9*, 6869–6881.

Singh, N., Sanyal, U., Ruehl, G., Stoerzinger, K.A., Gutiérrez, O.Y., Camaioni, D.M., Fulton, J.L., Lercher, J.A., and Campbell, C.T. (2020). Aqueous phase catalytic and electrocatalytic hydrogenation of phenol and benzaldehyde over platinum group metals. J. Catal. *382*, 372–384.

Stoerzinger, K.A., Favaro, M., Ross, P.N., Yano, J., Liu, Z., Hussain, Z., and Crumlin, E.J. (2018). Probing the surface of platinum during the hydrogen evolution reaction in alkaline electrolyte. J. Phys. Chem. B *122*, 864–870.

Stoerzinger, K.A., Hong, W.T., Crumlin, E.J., Bluhm, H., and Shao-Horn, Y. (2015). Insights into electrochemical reactions from ambient pressure photoelectron spectroscopy. Acc. Chem. Res. *48*, 2976–2983.

Sun, T., Yu, Y., Zacher, B.J., and Mirkin, M.V. (2014). Scanning electrochemical microscopy of individual catalytic nanoparticles. Angew. Chem. Int. Ed. *53*, 14120–14123.

Takahashi, I., Koga, O., Hoshi, N., and Hori, Y. (2002). Electrochemical reduction of CO_2 at copper single crystal Cu(S)-[n(111)×(111)] and Cu(S)-[n(110)×(100)] electrodes. J. Electroanalytical Chem. *533*, 135–143.

Tang, C., Shi, J., Bai, X., Hu, A., Xuan, N., Yue, Y., Ye, T., Liu, B., Li, P., Zhuang, P., et al. (2020). CO_2 reduction on copper's twin boundary. ACS Catal. *10*, 2026–2032.

Todoroki, N., Tei, H., Tsurumaki, H., Miyakawa, T., Inoue, T., and Wadayama, T. (2019). Surface atomic arrangement dependence of electrochemical CO_2 reduction on gold: online electrochemical mass spectrometric study on low-index Au(hkl) surfaces. ACS Catal. *9*, 1383–1388.

Vidal-Iglesias, F.J., Arán-Ais, R.M., Solla-Gullón, J., Herrero, E., and Feliu, J.M. (2012). Electrochemical characterization of shape-controlled Pt nanoparticles in different supporting electrolytes. ACS Catal. *2*, 901–910.

Wang, Y., Han, P., Lv, X., Zhang, L., and Zheng, G. (2018). Defect and interface engineering for aqueous electrocatalytic CO_2 reduction. Joule *2*, 2551–2582.

Yu, Y., Mao, B., Geller, A., Chang, R., Gaskell, K., Liu, Z., and Eichhorn, B.W. (2014). CO_2 activation and carbonate intermediates: an operando AP-XPS study of CO_2 electrolysis reactions on solid oxide electrochemical cells. Phys. Chem. Chem. Phys. *16*, 11633–11639.

Zalitis, C.M., Kucernak, A.R., Sharman, J., and Wright, E. (2017). Design principles for platinum nanoparticles catalysing electrochemical hydrogen evolution and oxidation reactions: edges are much more active than facets. J. Mater. Chem. A *5*, 23328–23338.

Zhang, C., Grass, M.E., Yu, Y., Gaskell, K.J., DeCaluwe, S.C., Chang, R., Jackson, G.S., Hussain, Z., Bluhm, H., Eichhorn, B.W., et al. (2012). Multielement activity mapping and potential mapping in solid oxide electrochemical cells through the use of *operando* XPS. ACS Catal. *2*, 2297–2304.

Zheng, J., Zhuang, Z., Xu, B., and Yan, Y. (2015). Correlating hydrogen oxidation/evolution reaction activity with the minority weak hydrogen-binding sites on Ir/C catalysts. ACS Catal. *5*, 4449–4455.

Zhu, S., Jiang, B., Cai, W.-B., and Shao, M. (2017). Direct observation on reaction intermediates and the role of bicarbonate anions in CO_2 electrochemical reduction reaction on Cu surfaces. J. Am. Chem. Soc. *139*, 15664–15667.

Zhu, S., Li, T., Cai, W.-B., and Shao, M. (2019). CO_2 electrochemical reduction as probed through infrared spectroscopy. ACS Energy Lett. *4*, 682–689.

Zhu, S., Wang, Q., Qin, X., Gu, M., Tao, R., Lee, B.P., Zhang, L., Yao, Y., Li, T., and Shao, M. (2018). Tuning structural and compositional effects in Pd–Au nanowires for highly selective and active CO_2 electrochemical reduction reaction. Adv. Energy Mater. *8*, 1802238.